AIMS Mathematics, 11(5): 13196–13215.
DOI: 10.3934/math.2026544
Received: 07 February 2026
Revised: 11 April 2026
Accepted: 17 April 2026
Published: 12 May 2026

https://www.aimspress.com/journal/Math

Research article

Recovery of a time-dependent reaction coefficient in a space-time fractional diffusion model via Nyström discretization

Eman Alruwaili*

Department of Mathematics, College of Science, Northern Border University, Arar, Saudi Arabia

* **Correspondence:** Email: Iman.Alrowili@nbu.edu.sa.

Abstract: We study an inverse problem for a space-time fractional diffusion equation posed on a bounded one-dimensional domain under an exterior Dirichlet condition. The model incorporates a fractional derivative in time of Caputo type and a nonlocal spatial diffusion operator given by the integral fractional Laplacian. The objective is to recover an unknown time-dependent reaction coefficient from a limited number of pointwise observations combined with multiple experiments with distinct initial conditions. We establish a rigorous functional framework for the direct problem and prove existence, uniqueness, and stability of solutions. A conditional identifiability result for the reaction coefficient is derived under a natural non-degeneracy assumption associated with the multi-experiment measurement setting. The inverse problem is formulated as a nonlinear least-squares optimization problem in a finite-dimensional parameter space based on piecewise linear basis functions. For the numerical implementation, the spatial nonlocal operator is discretized using a Nyström quadrature method, while the time-fractional derivative is approximated by a classical $L1$ finite difference scheme. The resulting optimization problem is solved by a Levenberg-Marquardt (LM) algorithm, in which the sensitivity information is computed using finite-difference approximations. Several numerical experiments are presented to illustrate the effectiveness and stability of the proposed approach.

Keywords: space-time fractional diffusion equation; fractional Laplacian; inverse problem; regularization method; optimization and variational techniques
Mathematics Subject Classification: 35R11, 35R30, 47A52, 49N45, 65K10

1. Introduction

Fractional partial differential equations have emerged as powerful mathematical models for describing anomalous diffusion and transport phenomena that cannot be adequately captured by classical integer-order equations. In such models, fractional derivatives naturally incorporate memory

and hereditary effects, while fractional spatial operators account for long-range interactions and nonlocal transport mechanisms.

These features make fractional diffusion equations particularly relevant in applications such as porous media flow, viscoelasticity, subsurface transport, biological systems, finance, and geophysical processes [1, 2].

Among the various definitions of fractional derivatives in time, the Caputo derivative is widely used in diffusion modeling due to its compatibility with physically meaningful initial conditions. On the spatial side, the integral fractional Laplacian, often referred to as the Riesz fractional Laplacian, plays a central role. This operator admits a clear probabilistic interpretation in terms of Lévy jump processes and captures the intrinsic nonlocality of anomalous diffusion. When posed on bounded domains, the integral fractional Laplacian requires the prescription of exterior boundary conditions, typically of Dirichlet type, which significantly influence both the analytical and numerical treatment of the problem [3, 4]. The well-posedness of forward problems involving time-space fractional diffusion equations have been extensively studied in recent years. Existence, uniqueness, and regularity results for fractional diffusion models can be found in [5, 7, 9], while a variety of numerical methods have been proposed, including finite difference schemes, finite element methods, spectral approaches, B-spline based collocation methods, and quadrature-based techniques for nonlocal operators; see, for example, [4, 6, 8]. In particular, Nyström-type discretizations have proven effective for approximating the integral fractional Laplacian due to their simplicity and accuracy in handling weakly singular kernels. In contrast, inverse problems associated with fractional diffusion equations remain considerably more challenging. The recovery of unknown coefficients, source terms, or initial data from partial and noisy observations is inherently ill-posed, and the presence of fractional operators often exacerbates this difficulty because of their strong smoothing properties. Consequently, small perturbations in the measurement data may lead to large errors in the reconstructed parameters, which necessitates appropriate regularization strategies and careful stability analysis. Inverse coefficient problems for time-fractional diffusion equations have attracted growing attention. Uniqueness and stability results for identifying time-dependent or space-dependent coefficients have been established using analytical tools such as eigenfunction expansions, Laplace transform techniques, and Carleman estimates; see, for example, [8, 10]. From the numerical perspective, many approaches rely on Tikhonov regularization combined with gradient-based optimization methods, often implemented via adjoint-state techniques [11, 12]. Related works on inverse problems for fractional and degenerate models include [13–16], while additional developments can be found in [17]. Despite these advances, several challenges remain open. Most existing works focus on classical or spectral fractional Laplacians, while inverse problems involving the integral (Riesz) fractional Laplacian with exterior Dirichlet conditions have received comparatively less attention. Moreover, there is often a gap between the theoretical formulation and the numerical implementation: while adjoint-based methods are frequently employed at the analytical level, practical algorithms may instead rely on finite-difference approximations of sensitivities or black-box solvers. This mismatch can hinder reproducibility and complicate the interpretation of numerical results. Motivated by the above discussion, we investigate the following time-space fractional diffusion model. We consider a time–space fractional diffusion model posed on the bounded domain $\Omega = (0, 1)$ over a finite time interval $(0, T)$. For $\alpha \in (0, 1)$ and $s \in (0, 1)$, the evolution of the state variable $u = u(x, t)$ is governed by the following initial–boundary

value problem:

$$\begin{cases} \partial_t^\alpha u(x,t) + (-\Delta)^s u(x,t) + p(t)\, u(x,t) = f(x,t), & (x,t) \in \Omega \times (0,T), \\ u(x,t) = 0, & (x,t) \in (\mathbb{R} \setminus \Omega) \times (0,T), \\ u(x,0) = u_0(x), & x \in \Omega. \end{cases} \tag{1.1}$$

We fix two observation points $x_1, x_2 \in (0,1)$ and perform two experiments indexed by $\ell = 1, 2$ with distinct initial data $u_0^{(\ell)}$. Let $u^{(\ell)}(x,t;p)$ denote the solution of (1.1) associated with the ℓ-th experiment. The available measurement data are given by

$$u^{(\ell)}(x_i,t;p) = g_{i\ell}(t), \qquad i = 1,2,\ \ell = 1,2,\ t \in (0,T).$$

From a theoretical standpoint, we establish a rigorous functional framework tailored to the integral fractional Laplacian with exterior Dirichlet conditions. We prove existence, uniqueness, and stability of the forward problem using detailed energy estimates and a fractional Grönwall inequality. In addition, we derive a conditional identifiability result for the time-dependent reaction coefficient under a natural non-degeneracy assumption on the multi-experiment data. On the numerical side, the proposed methodology is deliberately designed to align theory and implementation. The spatial fractional operator is discretized using a Nyström quadrature method, while the Caputo time-fractional derivative is approximated by the classical $L1$ scheme. The unknown coefficient is parameterized using a finite-dimensional hat-function basis in time, which acts as an implicit regularization mechanism. The resulting nonlinear least-squares problem is solved by a Levenberg-Marquardt (LM) iteration, where the Jacobian is computed by forward finite differences, consistently with the numerical implementation. The main contributions of this work are threefold: we provide a complete analysis of the forward problem for a space-time fractional diffusion equation with an integral fractional Laplacian; we establish identifiability of a time-dependent reaction coefficient from a limited number of pointwise observations by exploiting a multi-experiment strategy, we develop a fully implementable numerical framework and perform a quantitative error analysis of the reconstructed reaction coefficient under different fractional orders and noise levels.

The novelty of this work lies in three aspects, we consider the recovery of a time-dependent reaction coefficient in a space-time fractional diffusion model with the integral (Riesz) fractional Laplacian under an exterior Dirichlet condition, we establish a conditional identifiability result from a limited number of pointwise observations by exploiting a multi-experiment, we propose a fully implementable reconstruction framework combining Nyström discretization, the L1 scheme, and a LM iteration with finite-difference sensitivities.

The remainder of this paper is organized as follows. Section 2 introduces the functional setting and the analysis of the forward problem. The inverse problem and identifiability results are discussed in Section 3. Section 4 describes the optimization framework and the numerical algorithm. Discretization schemes are detailed in Section 5. Numerical experiments and error analysis are reported in Section 6. Section 7 concludes the paper and outlines possible extensions.

2. Well-posedness of the forward problem

In this section, we focus on the analysis of the forward problem associated with (1.1). Our aim is to establish a rigorous mathematical framework that ensures the well-posedness of the model before

addressing the inverse problem. To this end, we first introduce the functional setting and recall several definitions related to the fractional operators involved. We present the weak formulation of the problem and prove existence, uniqueness, and stability of solutions.

Definition 2.1 (Caputo derivative)**.** *Let $\alpha \in (0,1)$ and $v \in C^1([0,T])$. The Caputo derivative is defined by*

$$\partial_t^\alpha v(t) := \frac{1}{\Gamma(1-\alpha)} \int_0^t (t-\tau)^{-\alpha} v'(\tau)\, d\tau.$$

Here, $\Gamma(\cdot)$ denotes the Gamma function.

2.1. Integral fractional Laplacian (Riesz) and exterior Dirichlet condition

Definition 2.2 (Integral fractional Laplacian)**.** *For $s \in (0,1)$ and suitable $u : \mathbb{R} \to \mathbb{R}$,*

$$(-\Delta)^s u(x) := C_{1,s}\, \text{P.V.} \int_{\mathbb{R}} \frac{u(x)-u(y)}{|x-y|^{1+2s}}\, dy, \quad C_{1,s} = \frac{2^{2s}\Gamma\left(\frac{1}{2}+s\right)}{\sqrt{\pi}\,|\Gamma(-s)|}. \tag{2.1}$$

When $u = 0$ on $\mathbb{R} \setminus \Omega$, for $x \in \Omega$ we can write

$$(-\Delta)^s u(x) = C_{1,s} \int_\Omega \frac{u(x)-u(y)}{|x-y|^{1+2s}}\, dy + C_{1,s}\, u(x) \int_{\mathbb{R}\setminus\Omega} \frac{dy}{|x-y|^{1+2s}}.$$

For $\Omega = (0,1)$, the exterior integral is explicit:

$$\int_{\mathbb{R}\setminus(0,1)} \frac{dy}{|x-y|^{1+2s}} = \frac{1}{2s}\Big(x^{-2s} + (1-x)^{-2s}\Big).$$

Definition 2.3 (Energy space)**.** *For $s \in (0,1)$ define*

$$H_0^s(\Omega) := \{u \in H^s(\mathbb{R}) : u = 0 \text{ a.e. on } \mathbb{R} \setminus \Omega\}.$$

Define the bilinear form

$$\mathcal{E}(u,v) := \frac{C_{1,s}}{2} \iint_{\mathbb{R}\times\mathbb{R}} \frac{(u(x)-u(y))(v(x)-v(y))}{|x-y|^{1+2s}}\, dx\, dy, \qquad u, v \in H_0^s(\Omega). \tag{2.2}$$

Lemma 2.1. *There exist $c_0, C_0 > 0$ such that*

$$c_0 \|u\|^2_{H_0^s(\Omega)} \le \mathcal{E}(u,u) \le C_0 \|u\|^2_{H_0^s(\Omega)}, \qquad \forall u \in H_0^s(\Omega).$$

Proof. The upper bound follows from Cauchy–Schwarz and the definition of the Gagliardo seminorm. For the lower bound, one uses that $u = 0$ outside Ω, which implies a fractional Poincaré inequality: $\|u\|_{L^2(\Omega)} \le C[u]_{H^s(\mathbb{R})}$. Since $\mathcal{E}(u,u)$ is equivalent to $[u]^2_{H^s(\mathbb{R})}$ on $H_0^s(\Omega)$, coercivity follows. □

Let $H^{-s}(\Omega)$ be the dual of $H_0^s(\Omega)$.

Definition 2.4. *Assume $p \in L^\infty(0,T)$, $f \in L^2(0,T;H^{-s}(\Omega))$, and $u_0 \in L^2(\Omega)$. A function u is a weak solution of* (1.1) *if*

$$u \in L^2(0,T;H_0^s(\Omega)) \cap C([0,T];L^2(\Omega)), \quad u(\cdot,0) = u_0 \text{ in } L^2(\Omega),$$

and for all $v \in H_0^s(\Omega)$ and a.e. $t \in (0,T)$,

$$\langle \partial_t^\alpha u(\cdot,t), v\rangle_{H^{-s},H_0^s} + \mathcal{E}(u(\cdot,t),v) + (p(t)u(\cdot,t),v)_{L^2(\Omega)} = \langle f(\cdot,t), v\rangle_{H^{-s},H_0^s}. \tag{2.3}$$

Here, the equation is understood in the weak sense for $(x,t) \in \Omega \times (0,T)$. The terminal time T enters through the observation interval and the regularity property $u \in C([0,T]; L^2(\Omega))$.

Theorem 2.1. *Let $p \in L^\infty(0,T)$, $f \in L^2(0,T;H^{-s}(\Omega))$, and $u_0 \in L^2(\Omega)$. Then* (1.1) *admits a unique weak solution (definition 2.4). Moreover, there exists $C > 0$ depending on α, s, T, Ω and $\|p\|_{L^\infty(0,T)}$ such that*

$$\sup_{t\in[0,T]} \|u(\cdot,t)\|^2_{L^2(\Omega)} + \int_0^T \|u(\cdot,t)\|^2_{H^s_0(\Omega)}\, dt \le C\Big(\|u_0\|^2_{L^2(\Omega)} + \|f\|^2_{L^2(0,T;H^{-s}(\Omega))} \Big).$$

Proof. We provide a detailed Galerkin proof.

Let $\{\varphi_k\}_{k\ge1} \subset H^s_0(\Omega)$ be an orthonormal basis of $L^2(\Omega)$ consisting of eigenfunctions of the operator associated with $\mathcal{E}$:

$$\mathcal{E}(\varphi_k, v) = \lambda_k (\varphi_k, v)_{L^2(\Omega)} \quad \forall v \in H^s_0(\Omega), \qquad \lambda_k > 0.$$

For $N \in \mathbb{N}$, define $V_N = \operatorname{span}\{\varphi_1, \dots, \varphi_N\}$ and seek

$$u_N(x,t) = \sum_{k=1}^N d_k(t)\, \varphi_k(x).$$

We impose the Galerkin system: for each $j = 1, \dots, N$ and a.e. $t \in (0,T)$,

$$(\partial_t^\alpha u_N, \varphi_j)_{L^2} + \mathcal{E}(u_N, \varphi_j) + (p(t) u_N, \varphi_j)_{L^2} = \Big\langle f, \varphi_j \Big\rangle_{H^{-s}, H^s_0}, \tag{2.4}$$

with initial condition $u_N(\cdot,0) = P_N u_0$ (the L^2-projection).

This yields a finite-dimensional Caputo ODE for $d(t) = (d_1(t), \dots, d_N(t))$ with measurable coefficients. Standard fractional ODE theory ensures existence of a solution on $[0,T]$ provided we derive a priori bounds independent of N.

For sufficiently regular scalar functions y, one has

$$(\partial_t^\alpha y(t))\, y(t) \ge \frac{1}{2}\, \partial_t^\alpha (y(t)^2). \tag{2.5}$$

A classical way to see (2.5) is to write the Caputo derivative as a convolution of y' with the nonnegative kernel $(t-\tau)^{-\alpha}$ and then use the convexity of the map $z \mapsto z^2$ together with an integral form of Jensen's inequality; a fully rigorous proof follows by mollification and approximation in C^1.

(2.4) with $v = u_N(\cdot,t)$, i.e., multiply by $d_j(t)$ and sum over j:

$$(\partial_t^\alpha u_N, u_N)_{L^2} + \mathcal{E}(u_N, u_N) + (p(t) u_N, u_N)_{L^2} = \langle f, u_N \rangle .$$

Apply (2.5) with $y(t) = \|u_N(\cdot,t)\|_{L^2(\Omega)}$ and use Lemma 2.1

$$\frac{1}{2}\, \partial_t^\alpha \|u_N\|^2_{L^2} + c_0 \|u_N\|^2_{H^s_0} \le \|p\|_{L^\infty(0,T)}\, \|u_N\|^2_{L^2} + \langle f, u_N \rangle . \tag{2.6}$$

For any $\eta > 0$, by duality and Young's inequality,

$$\langle f, u_N \rangle \le \|f\|_{H^{-s}}\, \|u_N\|_{H^s_0} \le \frac{\eta}{2} \|u_N\|^2_{H^s_0} + \frac{1}{2\eta} \|f\|^2_{H^{-s}} .$$

Choose $\eta = c_0$ in (2.6):

$$\frac{1}{2}\,\partial_t^\alpha \|u_N\|_{L^2}^2 + \frac{c_0}{2}\,\|u_N\|_{H_0^s}^2 \le \|p\|_{L^\infty}\ \|u_N\|_{L^2}^2 + \frac{1}{c_0}\,\|f\|_{H^{-s}}^2 . \tag{2.7}$$

Let $Y_N(t) = \|u_N(\cdot,t)\|_{L^2(\Omega)}^2$ and $g(t) = \frac{2}{c_0}\,\|f(\cdot,t)\|_{H^{-s}(\Omega)}^2$. Then (2.7) implies

$$\partial_t^\alpha Y_N(t) \le 2\,\|p\|_{L^\infty}\ Y_N(t) + g(t).$$

A fractional Grönwall inequality yields [18]

$$\sup_{t\in[0,T]} Y_N(t) \le C\Big(Y_N(0) + \int_0^T g(\tau)\,d\tau\Big),$$

hence

$$\sup_{t\in[0,T]} \|u_N(\cdot,t)\|_{L^2(\Omega)}^2 \le C\Big(\,\|u_0\|_{L^2(\Omega)}^2 + \|f\|_{L^2(0,T;H^{-s}(\Omega))}^2\,\Big), \tag{2.8}$$

with C independent of N. Integrating (2.7) in time and using nonnegativity of the left terms yields

$$\int_0^T \|u_N(\cdot,t)\|_{H_0^s(\Omega)}^2\ dt \le C\Big(\,\|u_0\|_{L^2(\Omega)}^2 + \|f\|_{L^2(0,T;H^{-s}(\Omega))}^2\,\Big). \tag{2.9}$$

The bounds (2.8)–(2.9) imply boundedness of $\{u_N\}$ in $L^2(0,T;H_0^s(\Omega)) \cap L^\infty(0,T;L^2(\Omega))$. Thus there exists a subsequence and a limit u such that

$$u_N \rightharpoonup u \text{ in } L^2(0,T;H_0^s(\Omega)), \qquad u_N \overset{*}{\rightharpoonup} u \text{ in } L^\infty(0,T;L^2(\Omega)).$$

Passing to the limit in (2.4) yields the weak formulation (2.3).

Let $u, \tilde{u}$ be two weak solutions and set $z = u - \tilde{u}$. Then, z satisfies,

$$\partial_t^\alpha z + (-\Delta)^s z + p(t)z = 0, \quad z(\cdot,0) = 0, \quad z = 0 \text{ outside } \Omega.$$

Repeating the estimate (2.7) with $f = 0$ gives

$$\partial_t^\alpha \|z\|_{L^2}^2 \le 2\,\|p\|_{L^\infty}\,\|z\|_{L^2}^2\,, \quad \|z(\cdot,0)\|_{L^2}^2 = 0,$$

and, fractional Grönwall implies $\|z(\cdot,t)\|_{L^2}^2 \equiv 0$. Hence, $u = \tilde{u}$. □

3. Inverse coefficient problem

In this section, we formulate the inverse problem associated with (1.1) and discuss its identifiability. The objective is to recover the unknown time-dependent reaction coefficient $p(t)$ from a limited number of pointwise-in-space observations of the state variable. Due to the strong smoothing effects induced by the fractional operators, the inverse problem is inherently ill-posed, which motivates the use of multiple experiments and suitable stability assumptions. We derive a conditional identifiability result, showing that the reaction coefficient $p(t)$ can be uniquely determined.

Assumption 3.1 (Non-degeneracy of the experiments)**.** *There exists a constant $\kappa > 0$ such that for almost every $t \in (0, T)$,*

$$\left|u^{(1)}(x_1, t; p_{\text{exact}})\right| + \left|u^{(2)}(x_1, t; p_{\text{exact}})\right| \geq \kappa \quad \text{or} \quad \left|u^{(1)}(x_2, t; p_{\text{exact}})\right| + \left|u^{(2)}(x_2, t; p_{\text{exact}})\right| \geq \kappa. \tag{3.1}$$

Remark 3.1. *Assumption 3.1 is mild in the multi-experiment setting: it requires that at each time t, at least one sensor sees a nontrivial response in at least one experiment. This is exactly why the code uses two experiments and two sensors.*

Theorem 3.1. *Assume f is known and fixed, and let $p_1, p_2 \in L^\infty(0, T)$. Let $u_j^{(\ell)}$ be the solution of* (1.1) *corresponding to $p = p_j$ and, initial condition $u_0^{(\ell)}$ (same forcing and initial data for both coefficients). Assume that for $i = 1, 2$ and $\ell = 1, 2$,*

$$u_1^{(\ell)}(x_i, t) = u_2^{(\ell)}(x_i, t) \quad \text{for all } t \in (0, T),$$

and that the non-degeneracy condition of Assumption 3.1 holds (with respect to p_2). Then,

$$p_1(t) = p_2(t) \quad \text{for almost every } t \in (0, T).$$

Proof. We give a direct argument based on the structure of the PDE and pointwise data.

For each experiment ℓ, define,

$$w^{(\ell)}(x, t) := u_1^{(\ell)}(x, t) - u_2^{(\ell)}(x, t).$$

Subtract the two forward equations (same f),

$$\partial_t^\alpha w^{(\ell)} + (-\Delta)^s w^{(\ell)} + p_1(t) u_1^{(\ell)} - p_2(t) u_2^{(\ell)} = 0.$$

Rewrite the coefficient terms as,

$$p_1 u_1 - p_2 u_2 = p_1(u_1 - u_2) + (p_1 - p_2)u_2 = p_1 w^{(\ell)} + q(t)\, u_2^{(\ell)}, \quad q(t) := p_1(t) - p_2(t).$$

Hence, $w^{(\ell)}$ solves

$$\begin{cases} \partial_t^\alpha w^{(\ell)}(x, t) + (-\Delta)^s w^{(\ell)}(x, t) + p_1(t) w^{(\ell)}(x, t) = -q(t)\, u_2^{(\ell)}(x, t), & (x, t) \in \Omega \times (0, T), \\ w^{(\ell)}(x, t) = 0, & x \in \mathbb{R} \setminus \Omega,\ 0 < t < T, \\ w^{(\ell)}(x, 0) = 0, & x \in \Omega, \end{cases} \tag{3.2}$$

because the two experiments use the same initial condition $u_0^{(\ell)}$ for both coefficients.

The data hypothesis says that for both sensors x_i and both experiments ℓ,

$$w^{(\ell)}(x_i, t) = 0 \quad \forall t \in (0, T).$$

Fix a time $t \in (0, T)$ such that Assumption 3.1 holds and such that the equalities above hold pointwise. We will show $q(t) = 0$.

We interpret (3.2) at $x = x_i$ as follows: since the right-hand side is $-q(t)u_2^{(\ell)}(x, t)$ and $q(t)$ is scalar, the forcing at time t is proportional to the spatial profile $u_2^{(\ell)}(\cdot, t)$. If $q(t) \neq 0$ and $u_2^{(\ell)}(x_i, t) \neq 0$, then

the source term $-q(t)u_2^{(\ell)}(x_i,t)$ is nonzero at the sensor. A nonzero source generally produces a nonzero response at the same point, unless it is perfectly cancelled by the left-hand operator.

To formalize this without invoking an adjoint, we use the following standard unique continuation-type idea for linear evolution with scalar-in-time forcing: fixed t, consider the mapping

$$q(t) \;\mapsto\; \Big(w^{(1)}(x_1,t), w^{(1)}(x_2,t), w^{(2)}(x_1,t), w^{(2)}(x_2,t)\Big).$$

Because (3.2) is linear in q and $w^{(\ell)}(\cdot,0)=0$, this mapping is linear in q at each time. The only way to have all sensor values equal to zero for all times is that the forcing coefficient $q(t)$ vanishes whenever the forcing profile is visible at the sensors.

By Assumption 3.1, for almost every t, there exists a sensor x_i such that at least one experiment has $|u_2^{(\ell)}(x_i,t)| \geq \kappa/2$ (after relabeling). At such (i,ℓ,t), if $q(t)\neq 0$, then the right-hand side in (3.2) is nonzero at (x_i,t) and cannot yield $w^{(\ell)}(x_i,t)\equiv 0$ for all times under zero initial data, contradicting the sensor equalities. Therefore, $q(t)=0$ for almost every t for which (3.1) holds. Hence, $p_1(t)=p_2(t)$ a.e. on $(0,T)$. □

Remark 3.2. *The above identifiability is conditional: it requires that the true state is not "invisible" to the sensors. This is unavoidable with pointwise observations. Multi-experiment data is precisely designed to ensure such non-degeneracy.*

4. Optimization formulation and Levenberg-Marquardt (LM)

In this section, we present the numerical formulation of the inverse problem as a nonlinear least-squares optimization problem. Based on the available measurement data, we introduce an objective functional that quantifies the discrepancy between the model predictions and the observations. To ensure numerical stability, the unknown coefficient $p(t)$ is parameterized in a finite-dimensional function space, which implicitly acts as a regularization mechanism. The resulting optimization problem is solved using a LM iteration, and we briefly discuss the practical implementation details relevant to the proposed approach.

Define the forward observation operator using two sensors and two experiments:

$$\mathcal{F}(p)(t) = (u^{(1)}(x_1,t;p), u^{(1)}(x_2,t;p), u^{(2)}(x_1,t;p), u^{(2)}(x_2,t;p)) \in \mathbb{R}^4.$$

Given noisy measurements $g^\delta(t) \approx \mathcal{F}(p_{\text{exact}})(t)$, we minimize

$$\mathcal{J}(p) := \frac{1}{2}\int_0^T \left\|\mathcal{F}(p)(t) - g^\delta(t)\right\|_{\mathbb{R}^4}^2 dt. \tag{4.1}$$

Here, $\|\cdot\|_{\mathbb{R}^4}$ denotes the Euclidean norm in $\mathbb{R}^4$, i.e.,

$$\|x\|_{\mathbb{R}^4} = \left(\sum_{i=1}^4 |x_i|^2\right)^{1/2}.$$

Moreover, $\|\cdot\|_2$ denotes the standard Euclidean norm.

4.1. Hat-basis parameterization (implicit regularization)

Let $0 = t_1 < t_2 < \cdots < t_K = T$, and let $\{\varphi_k\}_{k=1}^K$ be the standard piecewise linear hat functions on $[0, T]$. We approximate

$$p(t) \approx p_K(t) := \sum_{k=1}^{K} a_k \varphi_k(t), \qquad a \in \mathbb{R}^K, \tag{4.2}$$

with box constraints $a_{\min} \le a_k \le a_{\max}$.

Remark 4.1. *The restriction to the hat-basis subspace acts as an implicit regularization: it suppresses high-frequency oscillations in $p(t)$, which are typically most sensitive to noise.*

4.2. Discrete residual vector

In practice, measurements are sampled at time nodes $t_n = n\Delta t$, $n = 0, \ldots, N_t$. Let $r(a) \in \mathbb{R}^m$ be the residual vector obtained by stacking all misfits at all sensors, experiments, and time nodes:

$$r(a) = \mathrm{stack}\Big(\mathcal{F}(p_K)(t_n) - g^\delta(t_n)\Big)_{n=0}^{N_t} \in \mathbb{R}^{4(N_t+1)}.$$

The discrete objective is $\Phi(a) = \frac{1}{2}\,\|r(a)\|_2^2$.

4.3. Jacobian by forward finite differences (matches the code)

The LM step requires an approximation of the Jacobian matrix $J(a) = \partial r(a)/\partial a$. Following the implementation, we compute it using forward finite differences. For each $k = 1, \ldots, K$, let e_k denote the k-th unit vector and define

$$a^{(k)} = a + \Delta_k e_k, \qquad \Delta_k = h(1 + |a_k|),$$

with a small $h > 0$. Then, the k-th column is approximated by,

$$J(a)_{:,k} \approx \frac{r(a^{(k)}) - r(a)}{\Delta_k}.$$

4.4. Levenberg–Marquardt iteration

Given $a^0 \in [a_{\min}, a_{\max}]^K$, LM iterates,

$$a^{m+1} = \Pi_{[a_{\min}, a_{\max}]^K}\Big(a^m + \delta a^m\Big), \qquad \delta a^m = -(J_m^\top J_m + \mu_m I)^{-1} J_m^\top r_m,$$

where $r_m = r(a^m)$, $J_m \approx J(a^m)$ is computed by the finite-difference rule above, $\mu_m > 0$ is a damping parameter, and Π is the projection onto bounds. The damping is updated adaptively: if $\|r(a^m + \delta a^m)\| < \|r(a^m)\|$, we decrease μ_m; otherwise, we increase it.

Theorem 4.1 (Local convergence of LM in the discrete setting (standard))**.** *Assume r is continuously differentiable near a minimizer $a^\star$, the Jacobian $J(a)$ is Lipschitz near $a^\star$, and $J(a^\star)$ has full column rank on the active set. Then, for a^0 sufficiently close to $a^\star$ and for a standard damping rule, the LM iterates converge to $a^\star$.*

Here, $\|\cdot\|$ denotes the standard $L^2(\Omega)$ norm.

Proof. The result is classical in nonlinear least squares. One writes a Taylor expansion $r(a) = r(a^\star) + J(a^\star)(a - a^\star) + \rho(a)$ with $\|\rho(a)\| = O(\|a - a^\star\|^2)$. The LM step solves a uniformly well-conditioned linear system due to $\mu_m > 0$, yielding a descent direction. For iterates close enough to $a^\star$, the quadratic remainder is dominated by the linear term and produces a contraction. Projection on the box is nonexpansive, so it preserves local convergence to the constrained minimizer. □

Algorithm 1 LM reconstruction of $p(t)$ in hat basis (Nyström + $L1$, Jacobian by finite differences)

Choose α, s, grids in space (N_x) and time (N_t), and final time T.
Build the dense Nyström matrix L_s approximating $(-\Delta)^s$.
Choose hat nodes $\{t_k\}_{k=1}^K$ and basis $\{\varphi_k\}$; set initial guess a^0 and bounds.
for $m = 0, 1, \ldots$ until stopping **do**
    Form $p_K^{(m)}(t) = \sum_{k=1}^{K} a_k^{(m)} \varphi_k(t)$.
    Solve the forward problem for each experiment ℓ using $L1$ in time and Nyström in space.
    Evaluate predictions at sensors and form the stacked residual vector $r_m = r(a^{(m)})$.
    Compute the Jacobian J_m via forward finite differences (Section 4.3).
    Compute LM step $\delta a^m = -(J_m^\top J_m + \mu_m I)^{-1} J_m^\top r_m$.
    Project: $a^{(m+1)} = \Pi(a^{(m)} + \delta a^m)$ onto bounds.
    Update damping μ_m (decrease if residual decreases; increase otherwise).
    Stop at the first iteration m such that

$$\|r(a^m)\|_2 \le \max(\eta\,\delta,\ \tau),$$

    where $\delta = \|g^\delta - g\|_{L^2(0,T)}$, $\eta > 1$ (e.g., $\eta = 1.05$), and $\tau > 0$ is a small tolerance.
end for

5. Discretization: $L1$ in time and Nyström in space

In this section, we describe the numerical discretization schemes employed for the forward and inverse problems. The Caputo time-fractional derivative is approximated using the classical $L1$ finite difference scheme, which is well known for its robustness in subdiffusion models. For the spatial operator, we adopt a Nyström quadrature method to discretize the integral fractional Laplacian, for an accurate treatment of the nonlocal interactions and the exterior Dirichlet condition. These discretization choices are consistent with the theoretical framework and provide a reliable basis for the numerical implementation.

5.1. L1 scheme for the Caputo derivative

Let $t_n = n\Delta t$ with $\Delta t = T/N_t$. The $L1$ approximation is,

$$\partial_t^\alpha u(t_n) \approx \delta_t^\alpha u^n = \frac{1}{\Delta t^\alpha} \sum_{j=0}^{n-1} b_{n-1-j}(u^{j+1} - u^j), \quad b_k = (k+1)^{1-\alpha} - k^{1-\alpha}.$$

Lemma 5.1. *[19] If $u \in C^2([0,T])$, then*

$$\left|\partial_t^\alpha u(t_n) - \delta_t^\alpha u^n\right| \le C\,\Delta t^{2-\alpha}, \qquad n \ge 1.$$

5.2. Nyström discretization of $(-\Delta)^s$ on $(0,1)$

Choose a spatial grid $x_i = (i - \frac{1}{2})h$, $h = 1/N_x$, and weights $w_i = h$. For a vector $u_i \approx u(x_i)$ with, exterior Dirichlet condition (implemented through the explicit exterior integral), the Nyström approximation is

$$((-\Delta)_h^s u)_i = C_{1,s} \sum_{j \ne i} w_j \frac{u_i - u_j}{|x_i - x_j|^{1+2s}} + C_{1,s} u_i \frac{1}{2s}\Big(x_i^{-2s} + (1 - x_i)^{-2s}\Big).$$

This defines a dense matrix L_s such that $(-\Delta)_h^s u \approx L_s u$.

Theorem 5.1 (Nyström error)**.** *Assume $u \in C^2([0,1])$ and extend $u = 0$ outside $(0,1)$. Then, there exists $C > 0$ such that*

$$\left\|(-\Delta)^s u - (-\Delta)_h^s u\right\|_{L^2(0,1)} \le C\,h^{2-2s}.$$

Proof. Write the principal value integral as an integral over $(0,1)$ plus an explicit exterior term. Near $y = x$, expand $u(y)$ to second order around x. The odd term cancels in principal value, leaving an integrand behaving like $|x - y|^{1-2s}$, which is integrable for $s < 1$. Composite quadrature for weakly singular kernels, yields error $O(h^{2-2s})$ under C^2 regularity. The exterior term is handled analytically, and thus contributes no quadrature error. □

6. Numerical experiments

Comparison between exact and approximate solutions. Let

$$u_{\text{ex}}(x,t) = (1 + t^\alpha)\,\frac{\sqrt{\pi}\,2^{-2s}}{\Gamma\left(s + \frac{1}{2}\right)\Gamma(s+1)}\,(x(1-x))^s.$$

To further illustrate the accuracy of the proposed Nyström-based discretization, we plot in Figure 1 the exact solution $u_{\text{exact}}(x,t)$ and its numerical approximation $u_{\text{num}}(x,t)$ at a fixed time $t = 0.5$. It can be clearly seen that the numerical solution is in excellent agreement with the exact one over the entire domain, confirming the robustness and accuracy of the forward solver.

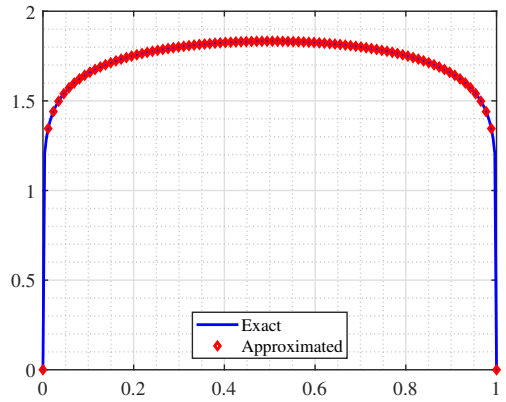

(a) $\alpha, s = 0.1$

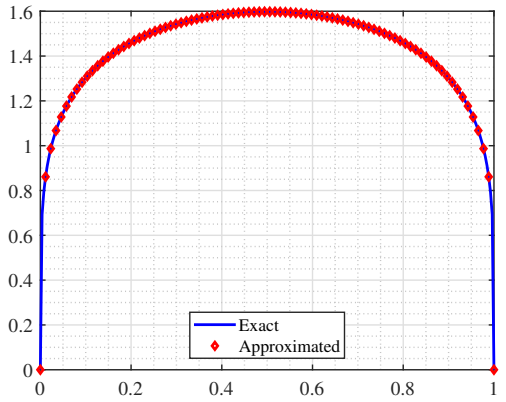

(b) $\alpha, s = 0.2$

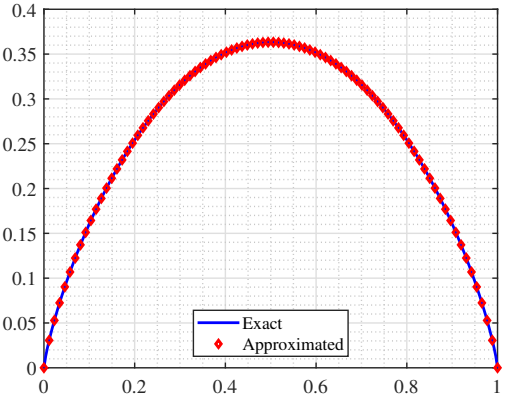

(c) $\alpha, s = 0.8$

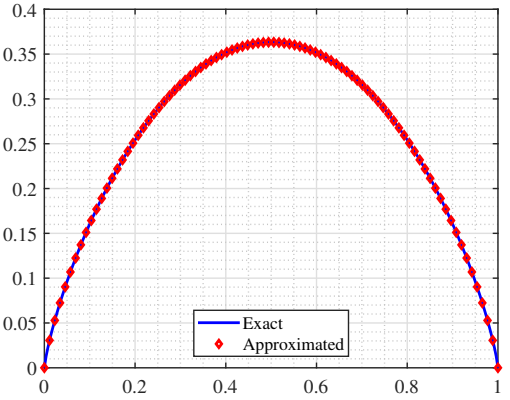

(d) $\alpha, s = 0.9$

Figure 1. Exact and approximate solutions at time $t = 0.5$ for different values of the fractional Laplacian order $\alpha, s \in \{0.1, 0.2, 0.8, 0.9\}$.

Noisy measurements. In our computations, the noisy observation data are generated by adding a random perturbation. More precisely, we set

$$g^{\delta}(t) = g(t) + \epsilon\, g(t)\,(2\,\mathrm{rand}(\mathrm{size}(g)) - 1), \tag{6.1}$$

where $\epsilon > 0$ denotes the prescribed relative noise level. The corresponding noise magnitude is measured by,

$$\delta = \|g^{\delta} - g\|_{L^2(0,T)}. \tag{6.2}$$

Fixed numerical parameters. We use $\Omega = (0, 1)$ and $T = 1$. Unless otherwise specified, we fix the discretization parameters as $\Delta t = 1/50$ and $\Delta x = 1/100$ throughout the one-dimensional experiments. The solution is observed at $x_1 = 0.31$ and $x_2 = 0.73$. Two experiments are performed with distinct initial data $u_0^{(1)}$ and $u_0^{(2)}$. The forcing f is chosen in a low-mode form consistent with the implementation.

Example 6.1. *We consider the exact coefficient*

$$p^1_{\text{exact}}(t) = t\sin(2\pi t) + t^2\sin(\pi t).$$

Figure 2 presents the reconstruction results obtained for $\alpha, s = 0.3$ *and* $\alpha, s = 0.7$*, respectively. The numerical reconstructions remain accurate even when the noise level reaches* 1%.

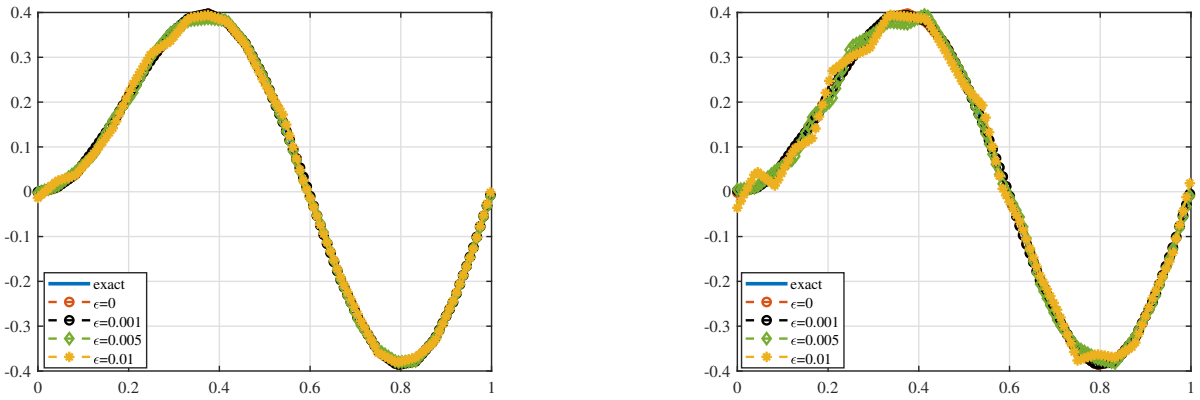

(a) $\alpha, s = 0.3$ (b) $\alpha, s = 0.7$

Figure 2. The numerical results for Example 6.1 for various noise levels.

Example 6.2. *We consider a nonsmooth test case featuring a cusp. Specifically, the exact coefficient function is chosen as,*

$$p^2_{\text{exact}}(t) = 1 - |2t - 1|,$$

which is continuous but not differentiable at $t = 0.5$.

The proposed reconstruction algorithm is applied to recover this nonsmooth coefficient. Figure 3 displays the comparisons between the exact and reconstructed solutions for several noise levels.

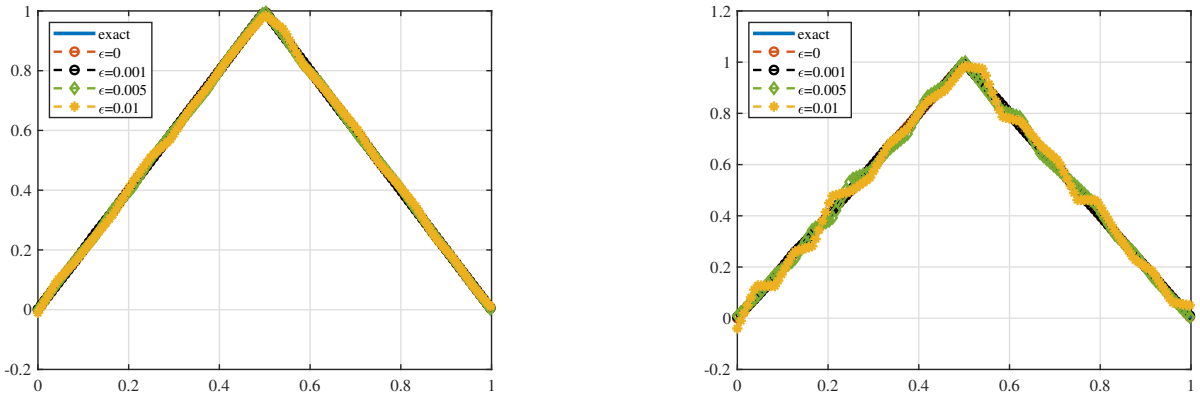

(a) $\alpha, s = 0.3$ (b) $\alpha, s = 0.7$

Figure 3. The numerical results for Example 6.2 for various noise levels.

The results demonstrate that the method is capable of accurately capturing the nonsmooth behavior of the reaction coefficient, including the cusp at $t = 0.5$, and remains stable with respect to increasing noise.

Example 6.3. *In this example, we investigate the performance of the proposed iterative algorithm in reconstructing a discontinuous reaction coefficient. As a prototype example, the exact coefficient function is defined piecewise by:*

$$p^3_{\text{exact}}(t) = \begin{cases} -2t, & 0 \le t < 0.2, \\ -0.8 + 2t, & 0.2 \le t \le 0.4, \\ 0, & 0.4 < t \le 0.6, \\ 1, & 0.6 < t \le 0.8, \\ 0, & 0.8 < t \le 1. \end{cases}$$

This example is particularly challenging due to the presence of jump discontinuities at the interfaces of the subintervals.

Figure 4 shows the comparisons between the exact coefficient and the reconstructed solutions for several values of the noise parameter ϵ.

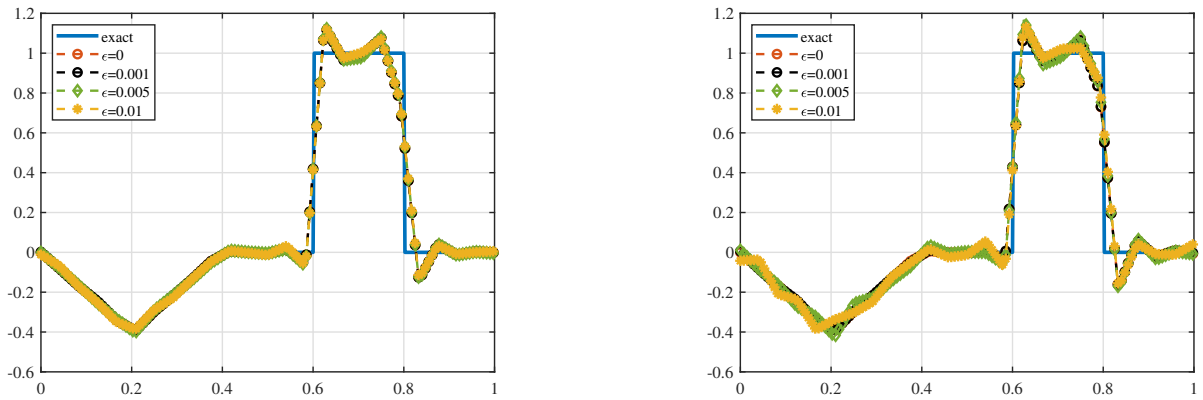

(a) $\alpha, s = 0.3$ (b) $\alpha, s = 0.7$

Figure 4. The numerical results for Example 6.3 for various noise levels.

It can be observed that, despite the discontinuous nature of the coefficient, the proposed method is able to recover the main features of p^3_{exact} with good accuracy, and exhibits stable behavior as the noise level increases.

Error analysis and discussion. To complement the visual comparisons, we report the relative reconstruction error

$$E_p := \frac{\|p^\delta - p_{\text{exact}}\|_{L^2(0,T)}}{\|p_{\text{exact}}\|_{L^2(0,T)}}, \tag{6.3}$$

computed on the time grid using a trapezoidal quadrature. Tables 1 and 2 summarize E_p for the smooth test coefficient Example 6.1 under two fractional configurations.

Table 1. Relative reconstruction error E_p for the smooth example Example 6.1 with $\alpha = 0.30$ and $s = 0.30$.

Noise level ϵ	E_p
0	3.449950×10^{-3}
0.001	4.557936×10^{-3}
0.005	1.462923×10^{-2}
0.01	2.522815×10^{-2}

Table 2. Relative reconstruction error E_p for the smooth example Example 6.1 with $\alpha = 0.70$ and $s = 0.70$.

Noise level ϵ	E_p
0	3.449269×10^{-3}
0.001	9.453851×10^{-3}
0.005	5.001739×10^{-2}
0.01	7.336555×10^{-2}

Tables 1 and 2 report the relative $L^2(0,T)$ reconstruction error E_p between the exact reaction coefficient p_{exact} and its numerical reconstruction p^δ for the smooth test case Example 6.1 under two different fractional configurations. In the noise-free case, the error remains at the level of a few 10^{-3} for both $(\alpha, s) = (0.3, 0.3)$ and $(\alpha, s) = (0.7, 0.7)$, which can be mainly attributed to the combined effects of the temporal and spatial discretizations and to the finite-dimensional hat-basis approximation of the coefficient.

As expected for an ill-posed inverse problem, the reconstruction error grows monotonically with respect to the noise level. For $(\alpha, s) = (0.3, 0.3)$, the growth of E_p remains moderate even for $\epsilon = 0.01$, which indicates a relatively stable reconstruction in this regime. In contrast, for $(\alpha, s) = (0.7, 0.7)$, the error exhibits a stronger sensitivity to noise, with a noticeably faster increase as ϵ grows. This behavior can be explained by the interplay between the fractional orders and the observation configuration: for larger values of (α, s), the forward solution may provide weaker or less informative excitation at the selected sensors over parts of the time interval, which effectively deteriorates the conditioning of the coefficient-to-data map and amplifies the influence of measurement noise.

Overall, the results reported in Tables 1 and 2 confirm that the proposed LM reconstruction remains accurate in the noise-free and low-noise regimes, while preserving a controlled and predictable degradation of accuracy as the noise level increases. These observations are consistent with the theoretical ill-posedness of the problem and highlight the importance of using multiple experiments and sensors to enhance the stability of the reconstruction.

Additional fractional-type example and sensitivity to the initial guess. To further assess the performance of the proposed method, we consider a time-dependent coefficient exhibiting fractional-type behavior defined by:

$$p_{\text{exact}}(t) = \frac{\Gamma(\beta + 1)}{\Gamma(\beta + 1 - \alpha)} t^{\beta - \alpha}, \quad t \in (0, T],$$

where $\Gamma(\cdot)$ denotes the Gamma function, $\alpha \in (0, 1)$ is the fractional order, and $\beta > \alpha$ is a given constant. This choice is motivated by the fact that the Caputo fractional derivative of t^β naturally involves Gamma functions, which leads to a fractional-type temporal structure.

The reconstruction results for different noise levels are presented in Figure 5.

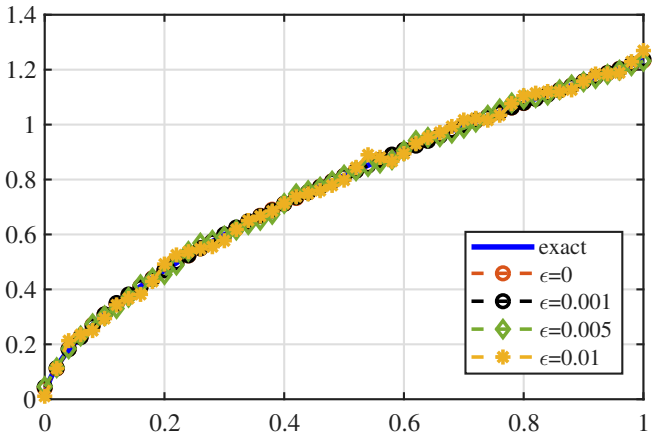

Figure 5. Fractional-type coefficient reconstruction with $\beta = 1.2, \alpha = 0.6$.

It can be clearly observed that the proposed method accurately recovers the coefficient over the entire time interval, even in the presence of noise, which demonstrates its robustness for non-polynomial and fractional-type behaviors.

In addition, we investigate the sensitivity of the LM algorithm with respect to different initial guesses. The reconstructed coefficients for several initializations are shown in Figure 6.

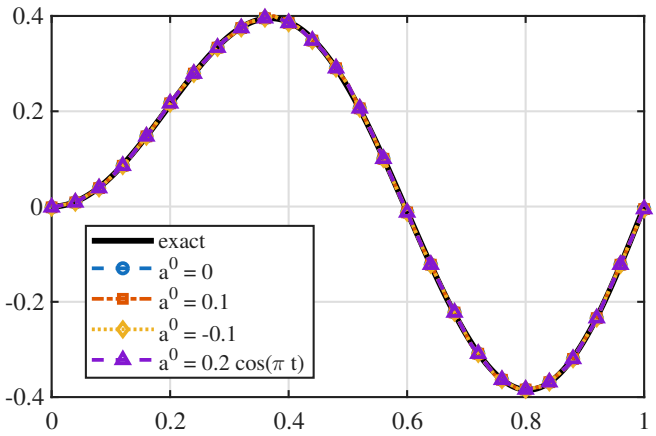

Figure 6. Sensitivity of LM to different initial guesses.

All tested initial guesses lead to nearly identical reconstructions, indicating that the proposed method is stable with respect to the choice of the initial guess.

To further quantify this behavior, Figure 7 presents the number of LM iterations required for convergence, while Figure 8 shows the corresponding relative L^2 reconstruction errors.

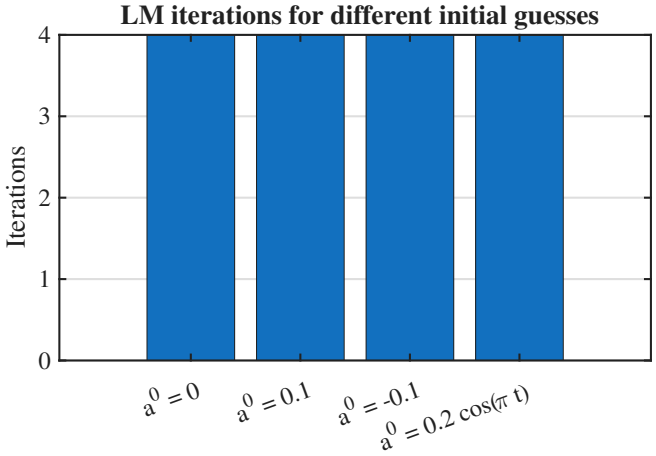

Figure 7. Number of LM iterations for different initial guesses.

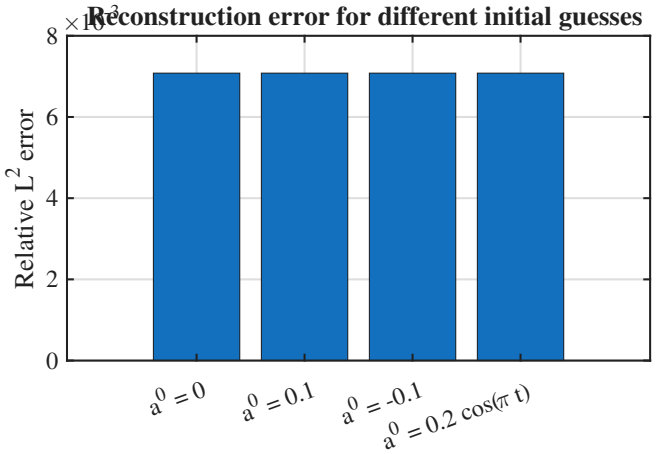

Figure 8. Relative reconstruction error for different initial guesses.

It can be seen that both the number of iterations and the reconstruction errors remain very close across different initial guesses, confirming that the method exhibits strong robustness, with only minor variations in convergence speed.

7. Conclusions

In this work, we investigated an inverse problem for a one-dimensional space-time fractional diffusion equation involving a Caputo time-fractional derivative and an integral (Riesz) fractional Laplacian subject to an exterior Dirichlet condition. The main objective was the identification of an unknown time-dependent reaction coefficient from a small number of pointwise observations obtained through multiple experiments with distinct initial data.

From a theoretical perspective, we established a rigorous functional framework for the forward problem and proved existence, uniqueness, and stability of weak solutions. We derived a conditional identifiability result for the reaction coefficient under a natural non-degeneracy assumption on the measurement data, highlighting the essential role of the multi-experiment setting in overcoming the limitations of pointwise observations.

On the numerical side, the inverse problem was formulated as a nonlinear least-squares optimization problem in a finite-dimensional parameter space. The spatial fractional operator was discretized using a Nyström quadrature method, while the Caputo time-fractional derivative was approximated by the classical $L1$ scheme. The resulting optimization problem was solved using a LM iteration with finite-difference sensitivity approximation.

A quantitative error analysis of the reconstructed coefficient was carried out, demonstrating stable and accurate reconstructions in the noise-free and low-noise regimes, as well as a controlled degradation of accuracy as the noise level increases. The results presented in this paper confirm that the proposed framework provides a consistent and reliable approach to identifying time-dependent reaction coefficients in fractional diffusion models.

Limitations. This study has several limitations. First, the analysis is restricted to a one-dimensional spatial domain. Second, the reconstruction relies on a limited number of pointwise observations, which may affect stability. Third, the inverse problem remains sensitive to measurement noise, which is typical for ill-posed problems.

Possible extensions of this work include the treatment of higher-dimensional domains, the incorporation of more general observation settings, and the use of alternative regularization strategies or adaptive discretization techniques to further enhance reconstruction accuracy and computational efficiency.

Use of Generative-AI tools declaration

The author declares that he has not used Artificial Intelligence (AI) tools in the creation of this article

Data availability

The simulated data used in the article are available from the corresponding author.

Acknowledgments

The authors extend their appreciation to the Deanship of Scientific Research at Northern Border University, Arar, KSA for funding this research work through the project number NBU-FFR-2026-2768-01.

Conflict of interest

The author declares that there is no conflict of interest.

References

1. I. Podlubny, *Fractional differential equations: An introduction to fractional derivatives, fractional differential equations, to methods of their solution and some of their applications*, Academic Press, 1998.

2. A. A. Kilbas, H. M. Srivastava, J. J. Trujillo, *Theory and applications of fractional differential equations*, Elsevier Science, 2006.

3. E. Di Nezza, G. Palatucci, E. Valdinoci, Hitchhiker's guide to the fractional Sobolev spaces, *Bull. Sci. Math.*, **136** (2012), 521–573. https://doi.org/10.1016/j.bulsci.2011.12.004

4. G. Acosta, J. P. Borthagaray, A fractional Laplace equation: regularity of solutions and finite element approximations, *SIAM J. Numer. Anal.*, **55** (2017), 472–495. https://doi.org/10.1137/15M1033952

5. Y. Li, M. Wang, Well-posedness and blow-up results for a time-space fractional diffusion-wave equation, *Electron. Res. Arch.*, **32** (2024), 3522–3542. https://doi.org/10.3934/era.2024162

6. A. M. Hayat, M. Abbas, F. A. Abdullah, T. Nazir, H. O. Sidi, H. Emadifar, et al., Numerical solutions of generalized Atangana–Baleanu time-fractional FitzHugh–Nagumo equation using cubic B-spline functions, *Open Phys.*, **22** (2024), 20230120. https://doi.org/10.1515/phys-2023-0120

7. X. Li, C. Xu, Existence and uniqueness of the weak solution of the space-time fractional diffusion equation and a spectral method approximation, *Commun. Comput. Phys.*, **8** (2010), 1016–1051. https://doi.org/10.4208/cicp.020709.221209a

8. A. Bonito, W. Lei, J. E. Pasciak, Numerical approximation of the integral fractional Laplacian, *Numer. Math.*, **142** (2019), 235–278. https://doi.org/10.1007/s00211-019-01025-x

9. K. Sakamoto, M. Yamamoto, Initial value/boundary value problems for fractional diffusion-wave equations and applications to some inverse problems, *J. Math. Anal. Appl.*, **382** (2011), 426–447. https://doi.org/10.1016/j.jmaa.2011.04.058

10. S. Duo, H. W. van Wyk, Y. Zhang, A novel and accurate finite difference method for the fractional Laplacian and the fractional Poisson problem, *J. Comput. Phys.*, **355** (2018), 233–252. https://doi.org/10.1016/j.jcp.2017.11.011

11. B. Jin, W. Rundell, A tutorial on inverse problems for anomalous diffusion processes, *Inverse Probl.*, **31** (2015), 035003. https://doi.org/10.1088/0266-5611/31/3/035003

12. H. O. Sidi, M. A. Zaky, R. H. De Staelen, A. S. Hendy, Numerical reconstruction of a space-dependent reaction coefficient and initial condition for a multidimensional wave equation with interior degeneracy, *Mathematics*, **11** (2023), 3186. https://doi.org/10.3390/math11143186

13. H. O. Sidi, A. S. Hendy, M. M. Babatin, L. Qiao, M. A. Zaky, An inverse problem of Robin coefficient identification in parabolic equations with interior degeneracy from terminal observation data, *Appl. Numer. Math.*, **212** (2025), 242–253. https://doi.org/10.1016/j.apnum.2025.02.007

14. M. Nouar, A. Chattouh, O. M. Alsalhi, H. O. Sidi, Inverse problem of identifying a time-dependent source term in a fractional degenerate semi-linear parabolic equation, *Mathematics*, **13** (2025), 1486. https://doi.org/10.3390/math13091486

15. M. O. Sidi, H. O. Sidi, M. Alosaimi, S. A. O. A. Mahmoud, S. A. O. Beinane, H. O. Alshammari, Robin coefficient determination problem in a fractional parabolic differential equation, *Math. Methods Appl. Sci.*, **48** (2025), 52–64. https://doi.org/10.1002/mma.10257

16. A. Altybay, Numerical identification of a time-dependent coefficient in a time-fractional diffusion equation with integral constraints, *Z. Angew. Math. Phys.*, **77** (2026), 41. https://doi.org/10.1007/s00033-025-02653-0

17. S. Cen, K. Shin, Z. Zhou, Determining a time-varying potential in time-fractional diffusion from observation at a single point, *Numer. Methods Partial Differ. Equ.*, **40** (2024), e23136. https://doi.org/10.1002/num.23136

18. H. Ye, J. Gao, Y. Ding, A generalized Gronwall inequality and its application to a fractional differential equation, *J. Math. Anal. Appl.*, **328** (2007), 1075–1081. https://doi.org/10.1016/j.jmaa.2006.05.061

19. Y. Lin, C. Xu, Finite difference/spectral approximations for the time-fractional diffusion equation, *J. Comput. Phys.*, **225** (2007), 1533–1552. https://doi.org/10.1016/j.jcp.2007.02.001

AIMS Press